Supplementary Figure 1

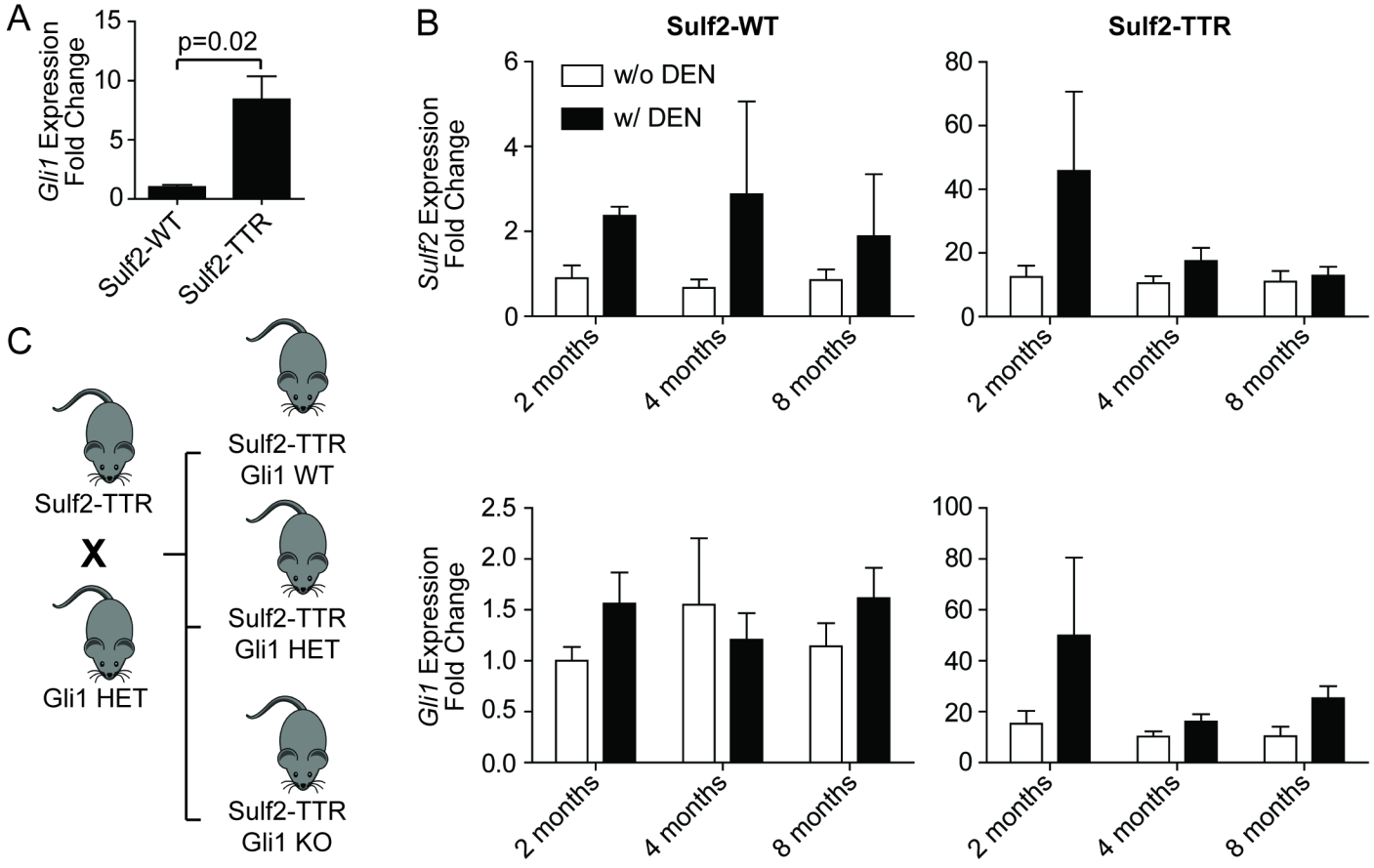

Supplementary Fig. 1

A. Assessment *Gli1* expression levels by qPCR in liver tissue derived from Sulf2-WT (n=3) and Sulf2-TTR (n=3) mice. Results are normalized to Sulf2-WT levels and expressed as means ± SEM. B. Determination of the effect of DEN treatment on *Sulf2* (above) and *Gli1* (below) expression levels by in liver tissue derived from 2 month, 4 month and 8 month old Sulf2-WT (left) and Sulf2-TTR (right) mice. This was assessed by qPCR and results are expressed as a mean of three replicates ± SEM. C. Schematic of genetic crosses between *Sulf2*-TTR mice and *Gli1* heterozygous knockout (HET) mice. Genotypes of interest are depicted including *Gli1* wildtype (WT), HET and knockout (KO) in the context of *Sulf2* overexpression (*Sulf2*-TTR).

Supplementary Figure 2

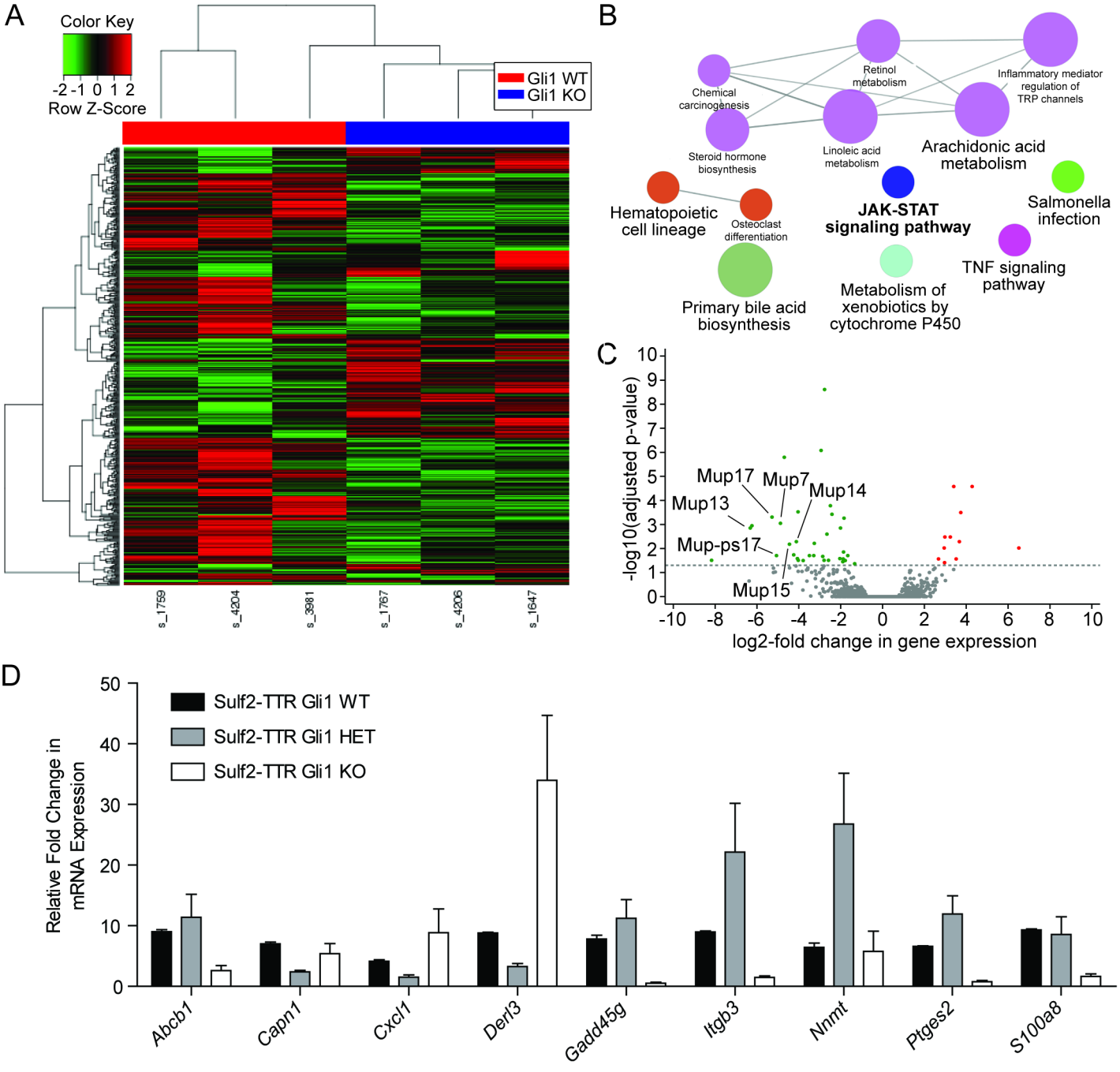

Supplementary Fig. 2

A. Heat map of RNA-seq results depicting clustering of transcriptomes of *Sulf2*-TTR, *Gli1* WT and *Gli1* KO mouse-derived tumors. B. KEGG pathway analysis of significantly downregulated genes in *Gli1* KO tumors relative to *Gli1* WT tumors. JAK-STAT signaling pathway is highlighted here. C. Replication of the volcano plot found in main figure 4. In this iteration, several downregulated major urinary proteins (Mup) are labeled. D. Validation of differential expression of putative Stat3 target genes by qPCR. This was conducted on RNA extracted from homogenized tumor tissue from the indicated mouse genotypes. Results are expressed as means ± SEM from three replicates.

Supplementary Figure 3

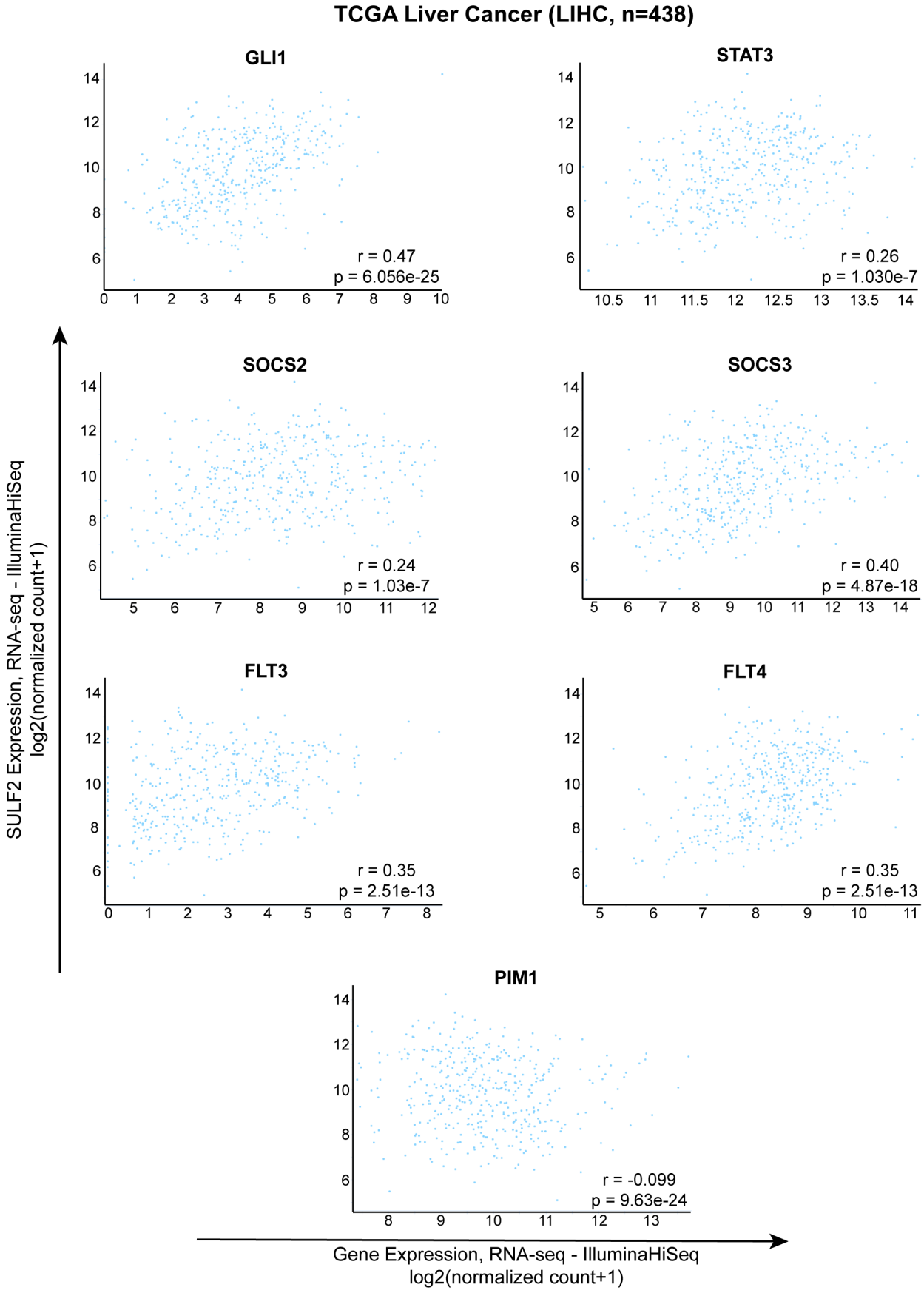

Supplementary Fig. 3

Data depicted in scatter plots are derived from RNA sequencing data from the liver cancer TCGA. Scatter plots compare expression of *SULF2* (y-axis) to each of the genes of interest (x-axis) expressed as log2(normalized count+1). Significance (p) and correlation (r) values for each comparison are indicated in the lower right of each plot.

Supplementary Figure 4

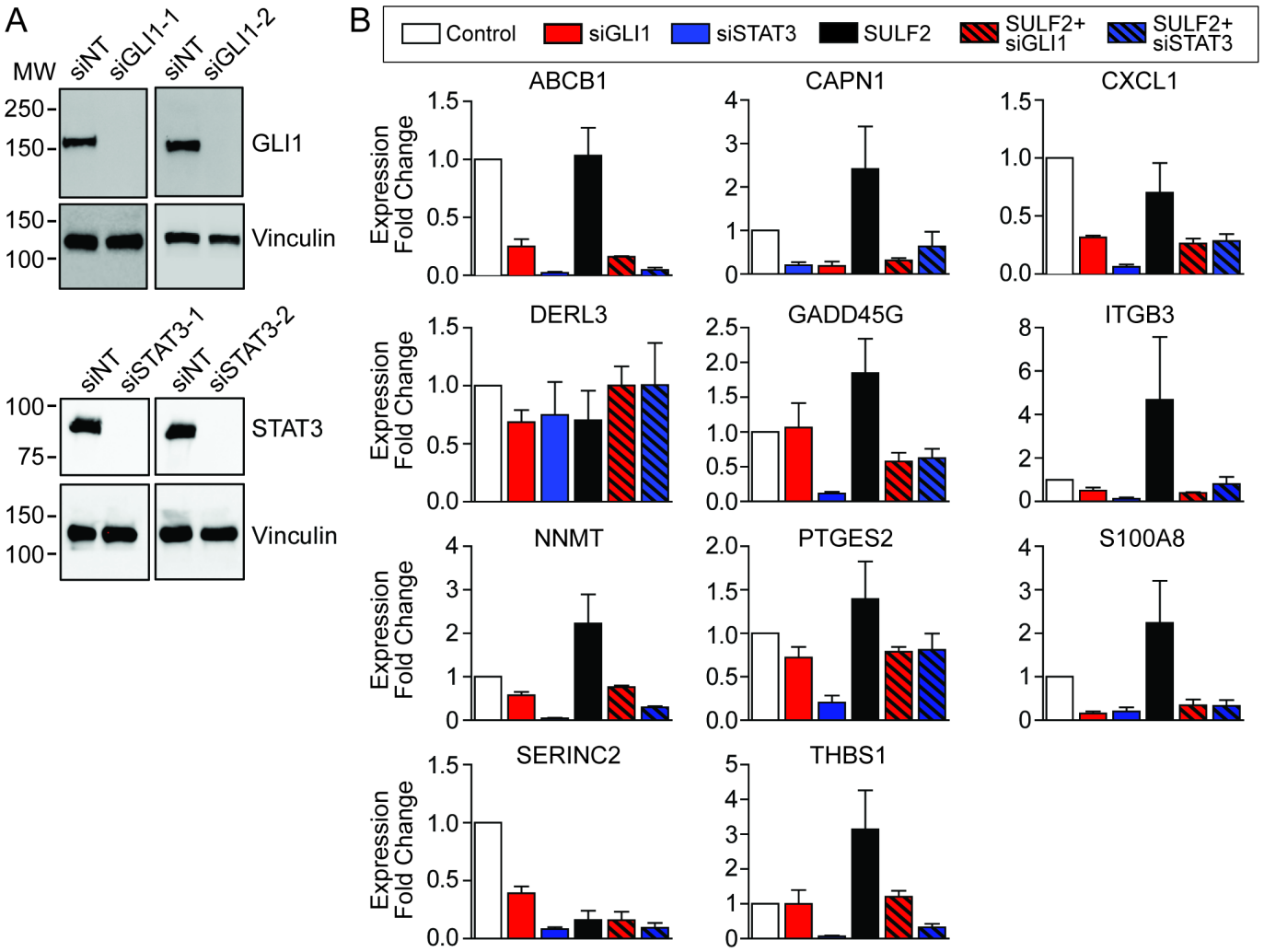

Supplementary Fig. 4

A. Western blots demonstrating transfection knockdown efficiency of GLI1 (above) and STAT3 (below) with two different siRNA constructs each. Vinculin was used as a loading control. Blots are representative of at least three independent experiments. MW indicates molecular weight presented in kilodaltons. B. Eleven genes potentially regulated by STAT3 identified as significantly downregulated with *Gli1* KO on RNA-seq analysis. Data represents results of qPCR performed on Huh-7 cells under the experimental conditions indicated. Cells were transfected with siNT, siGLI1 or siSTAT3 followed by transduction with either Adv-Null or Adv-SULF2. Results are expressed as means ± SEM from three replicates.

Supplementary Figure 5

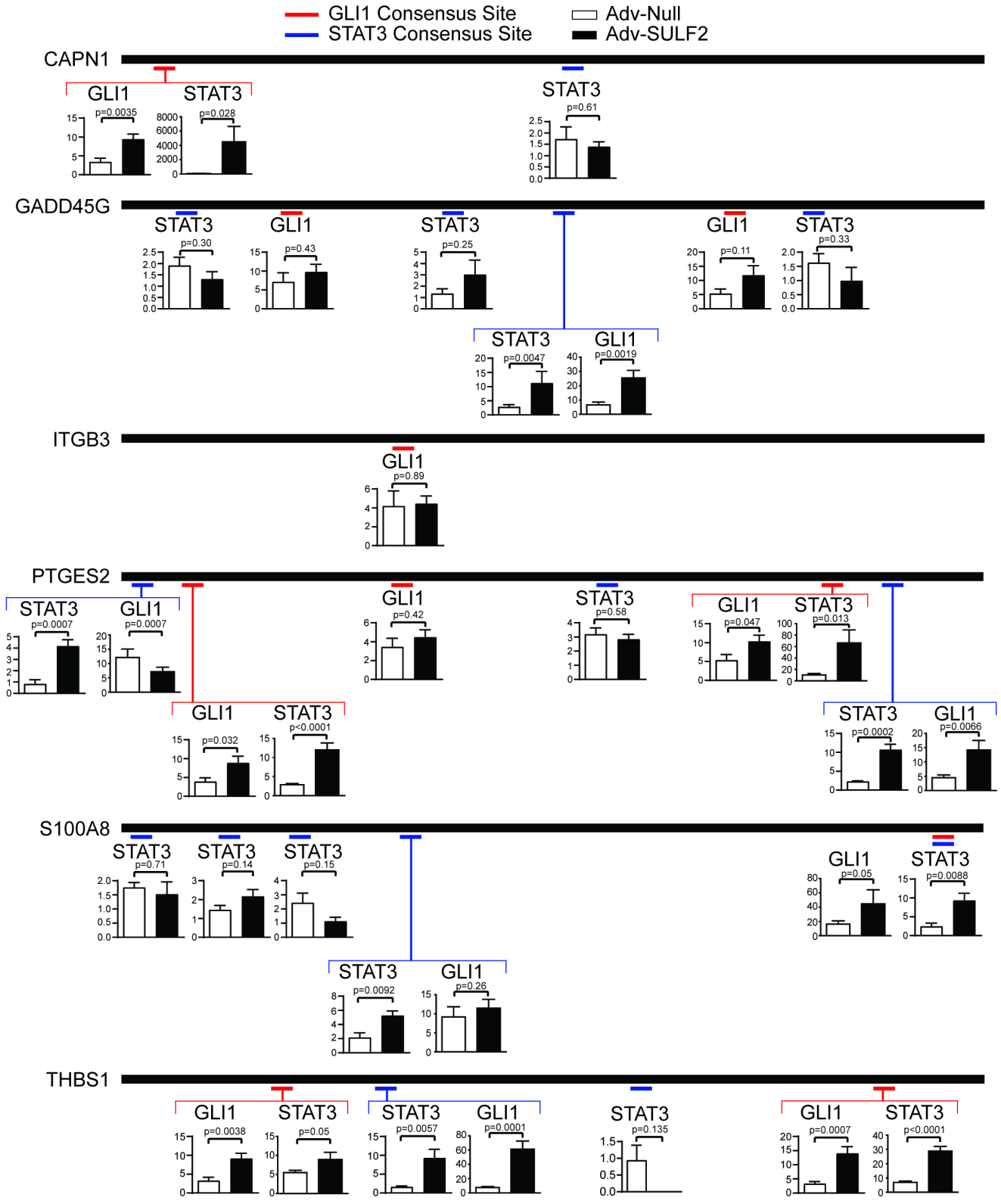

Supplementary Fig. 5

Depicted promoter maps representing the 300 nucleotides upstream of the TSS of putative STAT3-target genes identified on RNA-seq analysis. Relative positions of consensus binding sites for GLI1 (red) and STAT3 (blue) are depicted on the promoter maps. ChIP-PCR assays were performed on each of the potential transcription factor binding sites in Huh-7 cells transduced with either Adv-Null or Adv-SULF2. If GLI1 or STAT3 occupancy was significantly enriched with SULF2 expression relative to controls, ChIP-PCR was performed with immunoprecipitation of the reciprocal transcription factor. Results are expressed as means ± SEM from three replicates.